ACS APPLIED MATERIALS & INTERFACES

Research Article

www.acsami.org

Electrical Properties of Polypropylene-Based Composites Controlled by Multilayered Distribution of Conductive Particles

Wanli Gao, Yu Zheng, Jiabin Shen,* and Shaoyun Guo*

Polymer Research Institute of Sichuan University, State Key Laboratory of Polymer Materials Engineering, Chengdu, Sichuan 610065, P. R. China

ABSTRACT: Materials consisting of alternating layers of pure polypropylene (PP) and carbon black filled polypropylene (PPCB) were fabricated in this work. The electrical behaviors of the multilayered composites were investigated from two directions: (1) *Parallel to interfaces.* The confined layer space allowed for a more compact connection between CB particles, while the conductive pathways tended to be broken up with increasing number of layers leading to a distinct enhancement of the electrical resistivity due to the separation of insulated PP layers. (2) *Vertical to interfaces.* The alternating assemblies of insulated and conductive layers like a parallel-plate capacitor made the electrical conductivity become frequency dependent. Following the layer multiplication process, the dielectric permittivity was significantly enhanced due to the accumulation of electrical charges at interfaces. Thus, as a microwave was incident on the dielectric medium, the interfacial polarization made the main contribution to inherent dissipation of microwave energy, so that the absorbing peak became strengthened when the material had more layers. Furthermore, the layer interfaces in the multilayered system were also effective to inhibit the propagation of cracks in the stretching process, leading to a larger elongation at the break than that of the PP/CB conventional system, which provided a potential route to fabricate electrical materials with optimal mechanical properties.

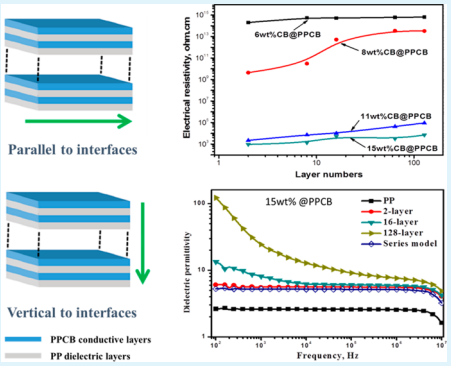

KEYWORDS: *conductive polymer composites, multilayered structure, interface, electrical properties, microwave absorption*

1. INTRODUCTION

With the pursuit of reduced size, lightweight, low cost, and high flexibility, microelectronic industries and portable smart devices create increasing demand for high performance conductive polymeric composites (CPCs).[1−3] However, most polymers are excellent electrical insulators, so that desired electrical conductivity is generally achieved through the addition of conductive particles, such as carbon black (CB),[4] carbon nanotube (CNT),[5] graphene,[6] carbon fiber (CF),[7] etc.

It is well-known that reducing the amount of conductive particles is one of the most crucial aspects in fabricating CPCs. Many investigations have focused on segregating those fillers from matrices into a confined continuous space, forming an efficient conductive network.[8−12] For example, Li and Shimizu[13] fabricated a poly(vinylidene fluoride) (PVDF)/polyamide 6 (PA6) blend with cocontinuous structure. When CNTs were located exclusively in the PA6 phase, the conductivity was increased by approximately 12 orders of magnitude. Gubbels et al.[14] showed a selective location of CB at the interfaces between polystyrene and polyethylene (PE) phases that form a cocontinuous blend dramatically reducing the amount of filled CB for percolation. Li et al.[15] prepared an in situ microfibrillar poly(ethylene terephthalate) (PET)/PE/CB conductive composite through hot stretching. The results indicated that CB-filled PET microfibrils could bridge each other, forming a conductive network and inducing a distinct decrease of the percolation threshold.

In fact, in the conventional blending system, the phase morphology and its continuity are controlled by various factors, including the concentration[16,17] and properties[18,19] of each component, the processing parameters,[20,21] etc. For example, a cocontinuous morphology can be attained within a narrow range of the ratio of components; the formation of the microfibrillar network is generally affected by the viscosity of the minor phase.[22] Hence, fabricating a stable and controllable continuous space for distributing conductive fillers has attracted much attention in the preparation of CPCs.

As a type of special cocontinuous morphology, the multilayered structure is regarded as a potential choice for fabricating CPCs. In a confined layer space, a smaller amount of conductive particles are required for percolation. Although the potential advantage of this unique structure has been discovered in electrical,[23] dielectric,[24,25] thermoelectric,[26] and microwave absorbing properties,[27] the influence of a controllable multilayered structure on these physical properties was rarely reported due to the limitation of fabricating methods, to the authors' best knowledge.

Recently, the emergence of a novel processing technology, layer-multiplying coextrusion, has made layer structures become more controllable and designable.[28,29] As schematically

Received: October 1, 2014
Accepted: December 30, 2014
Published: December 30, 2014

DOI: 10.1021/am506773c
ACS Appl. Mater. Interfaces 2015, 7, 1541−1549

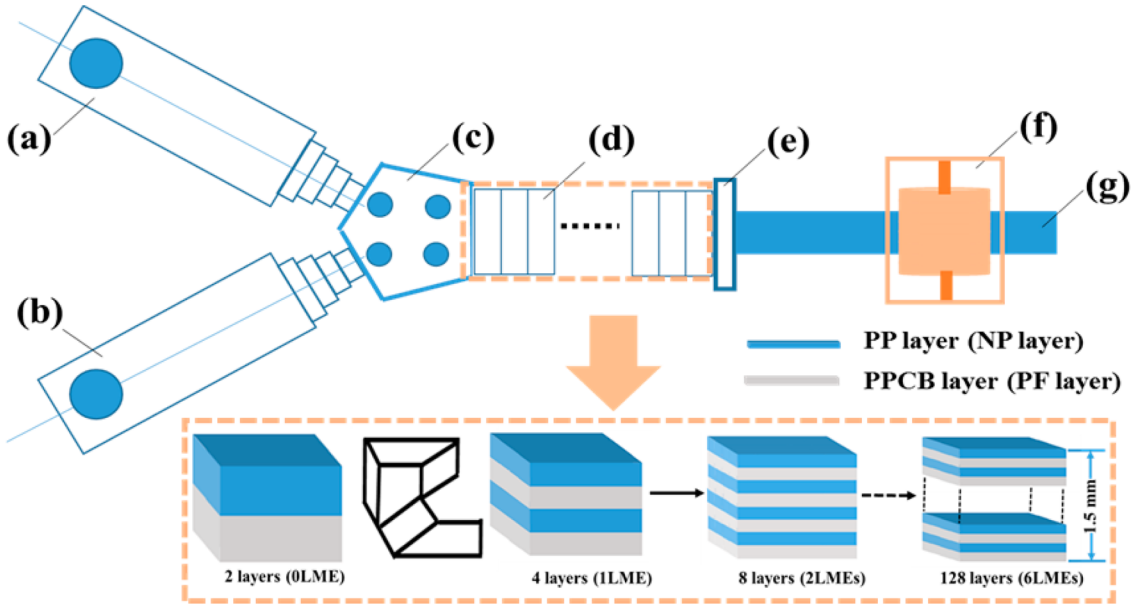

Figure 1. Schematic of layer-multiplying coextrusion system: (a,b) single screw extruder; (c) coextrusion block; (d) layer-multiplying elements (LMEs); (e) exit block; (f) rolling and cooling block; (g) extrudate.

illustrated in Figure 1, the multilayered CPC material consisting of alternating neat polymer (NP) layers and polymer/filler composite (PF) layers can be prepared by combining an assembly of layer-multiplying elements (LMEs) with two extruders. The number of layers can be multiplied by applying a different number of LMEs, without changing the overall thickness of the whole material. Since the conductive fillers are selectively distributed in PF layers, the multilayered material would exhibit an anisotropic conduction.

In this work, the multilayered CPC materials consisting of alternating polypropylene (PP) and CB-filled PP layers were fabricated. CB particles were chosen instead of other high aspect ratio fillers, such as CNTs, CFs, graphene, and metal fibers, to avoid the influence of the layer-multiplying process on the orientation of the conductive particles. This study intends to demonstrate the effectiveness of the confined distribution of conductive particles in alternating layers on electrical properties parallel and vertical to the interfaces of each specimen. Thus, other polymers, which can be melt-extruded, may be chosen as the matrix material instead of PP based on actual applications. Furthermore, the influence of the multilayered distribution of the conductive particles on mechanical properties of the polymer-based composite was also investigated.

2. EXPERIMENTAL SECTION

2.1. Materials. The isotactic PP (F401) used in this work was produced by Lan Zhou Petroleum Chemical Company Ltd. (China), with a density of 0.91 g/cm^3 and a melt index of 3 g/10 min. CB (E900) was obtained from Sichuan Zhenghao Special Carbon Technology Company Ltd. (China), with a density of 1.8 g/cm^3 and average particle size of 100−150 nm.

2.2. Specimen Preparation. Prior to layer-multiplying coextrusion, PP/CB pellets filled with 6, 8, 11, and 15 wt % CB particles were prepared using a twin-screw extruder (Nanjing Giant Co. Ltd., China), respectively.

PP/CB pellets and pure PP were coextruded through the layer-multiplying coextrusion technology, the mechanism of which has been described in previous work.[28,29] The multilayered composites consisting of alternating layers of pure PP and PP/CB (denoted as PPCB in the multilayered system) were fabricated with 2, 4, 16, 64, and 128 layers, respectively. By controlling the coextruding speed, the total thickness of each extrudate was about 1.5 mm, and the thickness ratio of PP and PPCB layers was maintained around 1:1. The CB contents in PPCB layers were 6, 8, 11, and 15 wt % (consistent with those in PP/CB pellets), thus the CB loadings in the whole multilayered composites were about 3, 4, 5, and 7 wt %, which were determined by thermogravimetric analysis, respectively.

For comparison, PP/CB conventional composites were also obtained. PP/CB pellets filled with 3, 4, 5, and 7 wt % CB particles were first prepared using a twin-screw extruder (Nanjing Giant Co. Ltd., China), respectively. Then, the PP/CB conventional composites were produced from one of the extruders of the layer-multiplying coextrusion system for keeping a processing history similar to the multilayered system. The thickness of each extrudate was 1.5 mm.

2.3. Morphological Observation. The polarized light microscope (PLM) observation was performed using an Olympus BX51 polarizing microscope equipped with a camera. A thin slice about 10 μm in thickness was obtained by a microtome from each sample perpendicular to the extruding direction.

The distribution of CB particles in multilayered specimens was observed using a scanning electron microscope (SEM, JEOL JSM-5900LV) under an accelerating voltage of 20 kV. Specimens were cryofractured in liquid nitrogen along a specific direction, and the fractured surface was coated with a layer of gold in a vacuum chamber prior to visualization by SEM.

2.4. Electrical Measurements. Considering the specific structure of the multilayered composites, the electrical properties were measured from two different directions.

(1). Parallel to Interfaces. Each specimen was cut from the center of an extruded sheet measuring 100.0 mm in length (l), 10.0 mm in width (w), and 1.5 mm in height (h). The contact faces were polished and coated by silver paste to eliminate the contact resistance between the sample edges and the electrode of the conduction tester. The electrical resistivity was measured on a programmable insulation resistance tester (YD9820A) consisting of a multivoltage source and a resistance meter. The constant voltage applied to the samples was fixed at 10 V. The electrical resistivity ($\rho_{\parallel}$) was calculated by the following equation

$$\rho_{\parallel} = R_V \frac{wh}{l}$$

where R_V was the electrical resistance. A minimum of five specimens were tested, and the average value was calculated.

DOI: 10.1021/am506773c
ACS Appl. Mater. Interfaces 2015, 7, 1541−1549

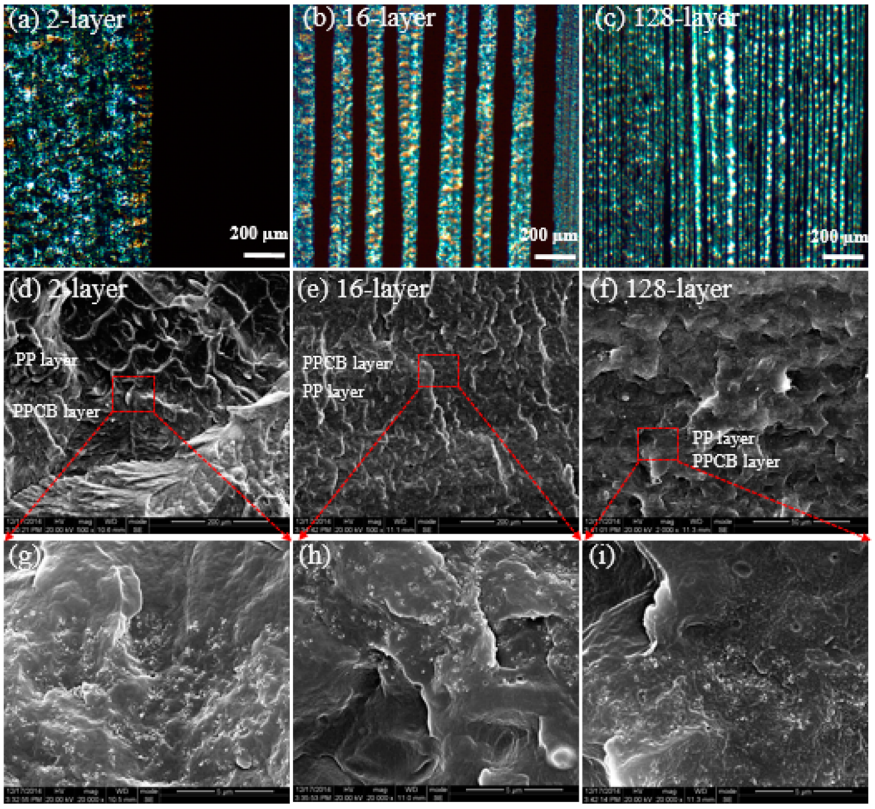

Figure 2. (a–c) PLM and (d–i) SEM morphological observation of PP/PPCB multilayered composites. (g), (h), and (i) are magnified images of the square zones in (d), (e), and (f).

Table 1. Electrical Resistivities of Two-Layer PP/PPCB Composites and PP/CB Conventional Composites

	two-layer PP/PPCB system					PP/CB conventional system
CB content in whole composites, wt %	CB content in PPCB layer, wt %	ρ_{PP}, Ω cm	ρ_{PPCB}, Ω cm	$\rho_{2L\text{-}cal}$, Ω cm	$\rho_{2L\text{-}exp}$, Ω cm	$\rho_{PP/CB\text{-}exp}$, Ω cm
3	6	9.4×10^{14}	5.3×10^{14}	3.4×10^{14}	2.0×10^{14}	6.3×10^{14}
4	8	9.4×10^{14}	1.2×10^{10}	1.2×10^{10}	4.4×10^{9}	5.9×10^{14}
5	11	9.4×10^{14}	7.3×10^{3}	7.3×10^{3}	2.2×10^{3}	5.0×10^{14}
7	15	9.4×10^{14}	8.0×10^{2}	8.0×10^{2}	9.2×10^{2}	3.8×10^{9}

(2). Vertical to Interfaces. Each specimen was cut from the center of an extruded sheet measuring 10.0 mm in length (l), 10.0 mm in width (w), and 1.5 mm in height (h). The voltage was applied on the thickness direction. I–V curves were measured by Keithley 4200. The applied voltage changed from 0 to 120 V with the interval of 1 V/s. To enhance the electrical contact between the samples and the electrodes, a silver paint was used.

2.5. Dielectric Measurements. Dielectric properties of each specimen in the thickness direction were measured using an Agilent 4294A impedance analyzer. The typical applied ac voltage was 1 V, and the test frequency range was 10^2–10^7 Hz. Prior to the tests, the contact faces of the specimen were coated with a conductive silver paste to eliminate contact resistance. The frequency-dependent conductivity and dielectric permittivity were obtained from the tests.

2.6. Microwave Absorption Measurements. The microwave-absorbing characteristics were evaluated by measuring the reflection loss using a vector network analyzer (VNA, Agilent 8720 ET) in the X band range (8.2–12.4 GHz). The sample sheets were mounted onto an aluminum substrate. All the measurements were performed at room temperature.

2.7. Tensile Tests. Tensile tests were performed using an Instron 4302 tension machine (Canton, MA, USA) at a crosshead speed of 20 mm/min in accordance with ASTM D638. At least five specimens for each sample were tested, and the average value was calculated.

3. RESULTS AND DISCUSSION

3.1. Microstructure. Figure 2(a–c) shows the microstructure of 2-, 16-, and 128-layer PP/PPCB composites (15 wt % CB @PPCB layers) obtained through PLM observations. The bright and dark layers, corresponding to PP and PPCB layers, are assembled alternately along the thickness direction of the specimen. With increasing the number of layers, numerous interfaces appear between PP and PPCB layers, while the thickness of each layer reduces proportionally since the total thickness of each specimen remains at 1.5 mm in the layer-multiplying process. By controlling the coextruding speed, the thickness ratio of PP and PPCB layers is close to 1:1. Thus, when the number of layers reaches 128, the average thickness of each layer is approximate to 12 μm, but CB particles are still confined in the PPCB layers and separated by neat PP layers. SEM observation was used to further reveal the distribution of CB particles in the multilayered specimens. As shown in Figure 2(d–f), the multilayered structure seems not as distinct as that observed through PLM. Figure 2(g–i) is magnified images of the square zones in Figure 2(d–f). It is clear that CB particles are located at one side of an interface, and the size of each CB

DOI: 10.1021/am506773c
ACS Appl. Mater. Interfaces 2015, 7, 1541–1549

aggregates remains around 1 μm even when the number of layers increases from 2 to 128.

3.2. Electrical Properties. *3.2.1. Parallel to Interfaces.* On the basis of the microstructure observed through microstructural observations, the resistivity of a two-layer PP/PPCB composite can be theoretically calculated according to the parallel-circuit model

$$\frac{1}{\rho_{2L}} = \frac{\varphi_{PPCB}}{\rho_{PPCB}} + \frac{\varphi_{PP}}{\rho_{PP}} \quad (1)$$

where φ_{PP} and φ_{PPCB} represent the volume fraction of PP and PPCB layers and ρ_{2L}, ρ_{PP}, and ρ_{PPCB} represent the electrical resistivities of the two-layer composite, PP, and PPCB layers, respectively. Because the insensitivity of ρ_{PP} and the thickness ratio of PP and PPCB layers in this work is 1:1, ρ_{2L} is mainly dependent on ρ_{PPCB}. Table 1 lists the calculated ($\rho_{2L\text{-cal}}$) and experimental ($\rho_{2L\text{-exp}}$) results of two-layer PP/PPCB specimens. It needs to be mentioned that the PPCB layers are loaded with four different CB contents, 6, 8, 11, and 15 wt %, corresponding to the cases below, near, and beyond the percolation threshold (P_c, 7.5 wt %) of the PP/CB conventional system. Distinctly, the calculated values are basically consistent with the measured ones, and the $\rho_{2L\text{-exp}}$ tends to get closer to ρ_{PPCB} with increasing content of conductive particles. Furthermore, Table 1 also compares the electrical resistivity of two-layer PP/PPCB composites and PP/CB conventional composites. In the two-layer system, CB was located in the PPCB layer. Hence, when the PPCB layer was combined with the PP layer, the CB contents in the two-layer composite were 3, 4, 5, and 7 wt %. In order to compare the electrical resistivity at the same CB contents, the PP/CB conventional specimens filled with the 3, 4, 5, and 7 wt % CB were also prepared, respectively. The results listed in Table 1 clearly display that the PP/CB conventional system has a much larger resistivity ($\rho_{PP/CB\text{-exp}}$) than that of the two-layer system ($\rho_{2L\text{-exp}}$). It indicates that the confined layer space allows for a more compact connection between conductive particles, promoting the formation of conductive pathways.

Further increasing the number of layers, the electrical resistivity of the PP/PPCB multilayered specimens (ρ_m) filled with different contents of conductive particles is displayed in Figure 3. When the CB loading in PPCB layers is below P_c, the electrical resistivity is basically maintained around 10^{14} Ω cm, irrespective of the layer numbers. However, for the materials filled with more CB particles, the electrical resistivity tends to rise up after the layer multiplication. This tendency becomes more obvious as the CB content in the PPCB layers reaches 8 wt %, near the P_c of the PP/CB conventional system. The resistivity of the 128-layer specimen is increased by approximately 4 orders of magnitude relative to the two-layer case, indicating that the original conductive network in PPCB layers is gradually broken up in the layer-multiplying process. When the CB contents in PPCB layers are beyond P_c, the effect of layer numbers on the electrical resistivity turns to become weakened, which suggests that the layer-multiplying process tends to have little influence on conductive pathways in PPCB layers as enough CB particles are loaded.

Similar to the two-layer case, the electrical resistivity of the PP/PPCB multilayered specimens (ρ_m) can also be theoretically calculated through the following equation according to the parallel-circuit model

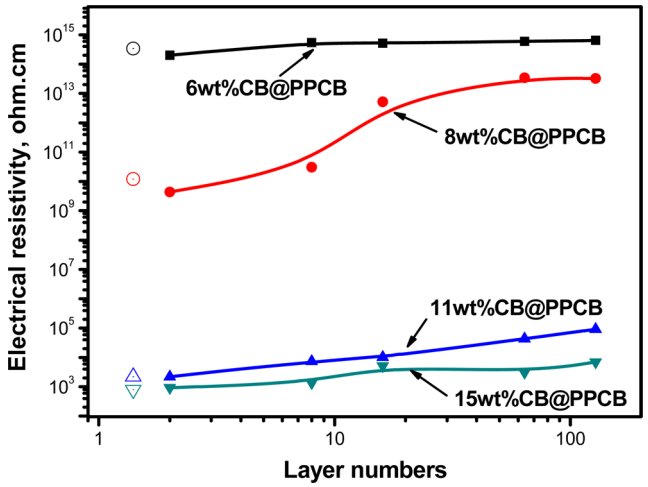

Figure 3. Electrical resistivity of PP/PPCB multilayered composites filled with different contents of CB as a function of layer numbers. The open symbols represent the calculated values based on the two-layer system.

$$\frac{1}{\rho_m} = \sum \frac{\varphi_{PPCB}}{\rho_{PPCB}} + \sum \frac{\varphi_{PP}}{\rho_{PP}} \quad (2)$$

Supposing that the ρ_{PPCB} is insensitive to the layer multiplication, ρ_m should be identical to ρ_{2L}. Thus, the calculated values of ρ_{2L} obtained from Table 1 are also marked as open symbols in Figure 3. It can be noticed that with increasing the number of layers the measured resistivity is basically larger than $\rho_{2L\text{-cal}}$, suggesting that the layer multiplication may result in the increase of ρ_{PPCB}. Besides, although there are only four kinds of CB contents, it can be speculated from Figure 3 that the conductive percolation threshold tends to become larger following the increase of layer numbers. It is also revealed that the layer-multiplying process plays a negative role in maintaining the original conductive network.

Actually, as CB particles are selectively distributed in PPCB layers, the conductive percolation of the whole multilayered system ($P_{c,m}$, wt %) depends on the percolation of CB in PPCB layers ($P_{c,CB}$, wt %) as well as the thickness ratio of PP and PPCB layers (φ), which can be regarded as a special "double percolation" effect.[30,31] In this work, φ almost equals one, thus the $P_{c,m}$ is mainly determined by $P_{c,CB}$ at different layer numbers. Figure 4 is a schematic of the development of conductive pathways in a PPCB layer with the increase of layer numbers. Ideally, the distribution of the conductive fillers is supposed to be uniform and stable in the layer-multiplying process. The dashed line in the PPCB layer is an imaginary interface that would be shared with a PP layer as the number of

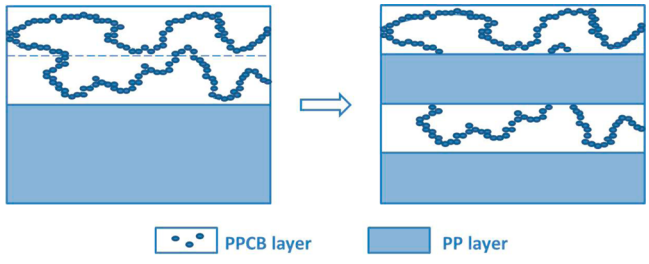

Figure 4. Schematic of the development of conductive pathways in a PPCB layer following the layer multiplication.

DOI: 10.1021/am506773c
ACS Appl. Mater. Interfaces 2015, 7, 1541−1549

layers doubles. Hence, the conductive pathways in a PPCB layer can be established by two routes (Figure 4 (left)): (1) CB particles within a pathway are completely above the imaginary line, the probability of which is χ_1; and (2) the conductive pathways can go through the imaginary line, the probability of which is χ_2. Thus, the total probability of the formation of conductive pathways χ equals $\chi_1 + \chi_2$. As the number of layers doubles (Figure 4 (right)), the PPCB layer is split along the dashed line, and an insulated PP layer is inserted. Thus, the conductive pathways originally going through the dashed line are cut off, such that χ_2 becomes zero and χ equals χ_1. This reveals that the layer multiplication may reduce the probability of conductive pathways being formed in PPCB layers leading to the increase of $P_{c,CB}$ as well as ρ_{PPCB}. Hence, in order to get a stable electrical resistivity, enough CB loadings are required for impeding the negative influence of the layer-multiplying process on the conductive pathways in PPCB layers. However, it needs to be highlighted that due to the double percolation effect induced from the multilayered distribution of conductive particles the material with a large number of layers still has a lower electrical resistivity than the PP/CB conventional composite. Taking 7 wt % CB-filled systems for example, the resistivity of the 128-layer PP/PPCB specimen (15 wt % CB in PPCB layers) is about 7×10^3 Ω cm, while that of the PP/CB conventional specimen is 3.8×10^9 Ω cm.

3.2.2. Vertical to Interfaces. Due to the multilayered distribution of CB in the polymeric matrix, anisotropic electrical properties parallel and vertical to the interfaces of a multilayered composite are distinct. For maintaining a stable electrical resistivity parallel to the interfaces, the CB loading in PPCB layers is fixed at 15 wt % (that means 7 wt % CB in the whole multilayered composite) in the following researches, based on Figure 3.

Figure 5 compares the electrical current of 2-, 16-, and 128-layer PP/PPCB specimens measured from 0 to 120 V. Result

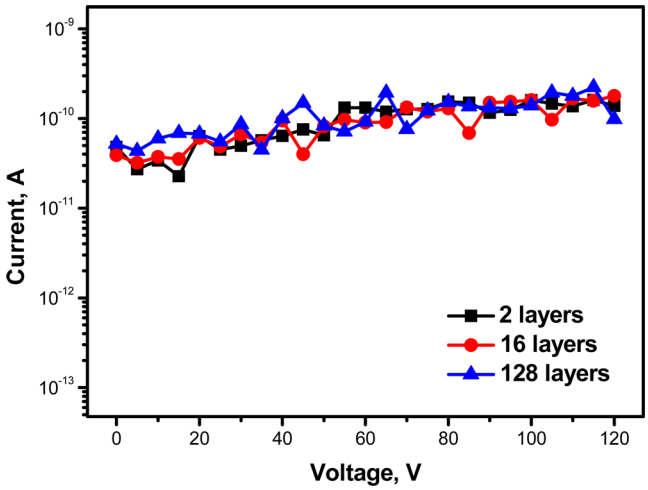

Figure 5. Electrical current of 2-, 16-, and 128-layer PP/PPCB specimens measured from 0 to 120 V.

shows that the current is almost maintained around 10^{-10} A with increasing the voltage, irrespective of the layer numbers. This reveals that due to the separation of insulated PP layers the multilayered system can be regarded as a "DC block" along its thickness direction, even when the number of layers reaches 128.

However, the alternating assembly of insulated and conductive layers can make the multilayered system perform like a parallel-plate capacitor. Figure 6 exhibits the frequency-

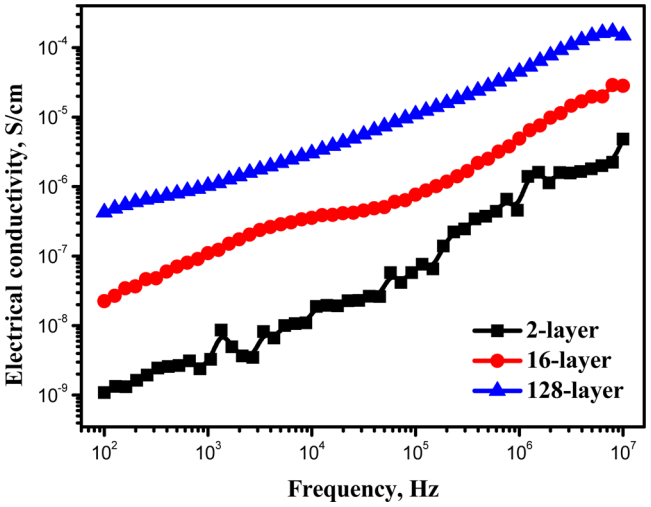

Figure 6. Electrical conductivity of 2-, 16-, and 128-layer PP/PPCB specimens as a function of frequency.

dependent conductivity ($\sigma(\omega)$) of the PP/PPCB composites with different number of layers. It can be observed that the conductivity of each specimen is increased by approximately 3 orders of magnitude from 10^2 to 10^7 Hz. As a higher frequency is applied, more electrical charges tend to be produced in a given period so that more current may be generated due to a lower capacitive reactance of the specimen, which is like a conventional capacitor.[32] Furthermore, the layer numbers also play a crucial role in $\sigma(\omega)$. At a given frequency, the conductivity of the 128-layer specimen is increased by approximately 2 orders of magnitude relative to the two-layer case. This indicates that the layer multiplication may promote the accumulation of electrical charges in the polarization process which can be further demonstrated based on the following results of dielectric permittivity.

As shown in Figure 7(a), the dielectric permittivity (ε) of pure PP and PP/PPCB multilayered composites was measured in the frequency range of 10^2 to 10^7 Hz, along the thickness direction under ambient temperature. For neat PP, the ε is almost maintained around 2.6 but starts to decrease as the frequency gets close to 10^7 Hz due to the polarization of molecular dipoles.[33] When the PP is combined with PPCB forming a two-layer specimen, the ε of the latter has a frequency dependence similar to that of pure polymer, but the value is almost doubled in the measured frequency range. According to the Series model of two-phase composites,[34] the permittivity of the PP/PPCB multilayered system (ε_c) can be described as follows

$$\frac{1}{\varepsilon_c} = \frac{\varphi_{PP}}{\varepsilon_{PP}} + \frac{\varphi_{PPCB}}{\varepsilon_{PPCB}}$$
$$\varphi_{PP} + \varphi_{PPCB} = 1 \quad (3)$$

where φ_{PP} and φ_{PPCB} represent the volume fraction of PP and PPCB layers, respectively. In this work, the content of CB in PPCB layers is 15 wt % far beyond the percolation threshold of PP/CB conventional composites. It is known that the ε of an ideal conductor tends to be infinity.[35] Hence, the ε_{PPCB} should

DOI: 10.1021/am506773c
ACS Appl. Mater. Interfaces 2015, 7, 1541−1549

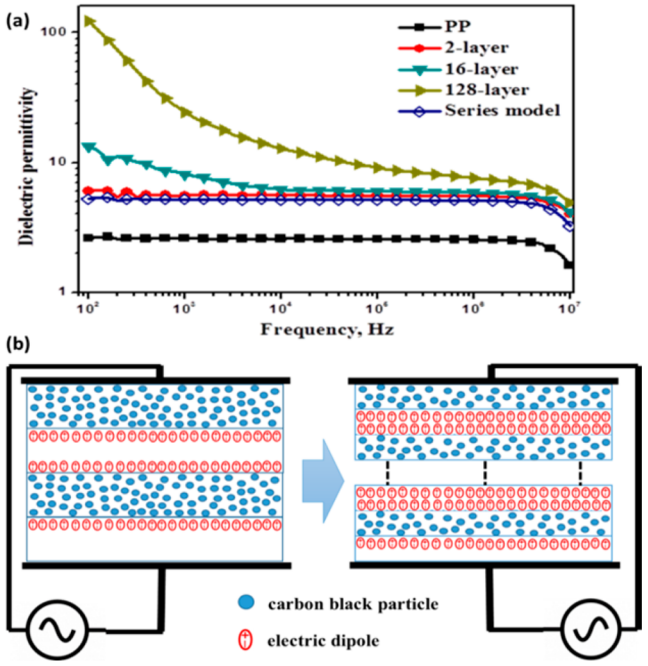

Figure 7. (a) Dielectric permittivity of pure PP and PP/PPCB multilayered specimens as a function of frequency. (b) Schematic of interfacial polarization occurring at interfaces of a multilayered specimen.

be much larger than ε_{PP}. Besides, the thickness ratio of PP and PPCB is about 1:1, so that the φ_{PP} equals to 0.5, and the equation can be simplified as follows

$$\frac{1}{\varepsilon_c} = \frac{1}{2\cdot\varepsilon_{PP}} \tag{4}$$

This means the ε_c would be two times the ε_{PP}, which is basically consistent with the experimental result of the two-layer specimen as shown in Figure 7(a). However, a larger enhancement of the permittivity is observed following the increase of the layer numbers. When the number of layers reaches 128, the ε at 10^2 Hz is almost 20 times higher than the predicted value based on the simplified Series model, which suggests that more charges can be polarized when conductive layers are alternately combined with insulated layers. It is known that when a frequency-dependent electric field is applied along the thickness direction of a specimen the voltage of each layer would be initially allocated by their capacitances and then gradually shift to be reallocated by the conductivity of each layer.[36] In this process, the electric charges would accumulate at the interfaces between adjacent layers as schematically illustrated in Figure 7(b). Thus, for a specimen with a large number of layers, more interfaces would be formed between PP and PPCB layers, which is considered to be beneficial to accelerate the interfacial polarization process so that more electrical charges tend to accumulate at interfaces leading to the distinct increase of the conductivity and dielectric permittivity.

3.3. Microwave Absorption. Numerous studies[37,38] have reported that dielectric properties commonly play crucial roles in microwave absorption of a shielding material, due to the interaction of microwave radiation with charge multipoles at the interfaces between conductive particles and the polymer matrix. Thus, the microwave absorption of the PP/PPCB multilayered composites induced by the multilayered distribution of CB was further considered in this work.

It is known that the microwave absorbing ability can be evaluated by measuring the reflection loss on a vector network analyzer.[39] A schematic representation of the measurement is shown in Figure 8(a). The specimen is placed on an aluminum substrate. The incident microwave is divided into two parts: the reflected microwave and the absorbed one. If P_{in} is the incident power density at a measuring point before absorption, P_{ref} is the reflected power density at the same point, and P_{abs} is the absorbed power by the specimen, then

$$P_{in} = P_{ref} + P_{abs} \tag{5}$$

$$RL = 10 \log \frac{P_{ref}}{P_{in}} \tag{6}$$

$$AL = 10 \log \frac{P_{abs}}{P_{in}} \tag{7}$$

where RL and AL represent the reflection loss and the absorption loss in decibels (dB), respectively. Commonly, the microwave absorbing efficiency is evaluated from RL.[40] The larger the absolute value of RL is, the stronger the wave-absorbing ability will be.

Figure 8(b) displays the RL plots of 2-, 16-, and 128-layer PP/PPCB composites at the X band between 8.2 and 12.4 GHz. For the two-layer specimen, it shows a weak absorbing ability, and the maximum value of RL (RL_{max}) is 12 dB. With increasing the number of layers, the absorbing peak becomes

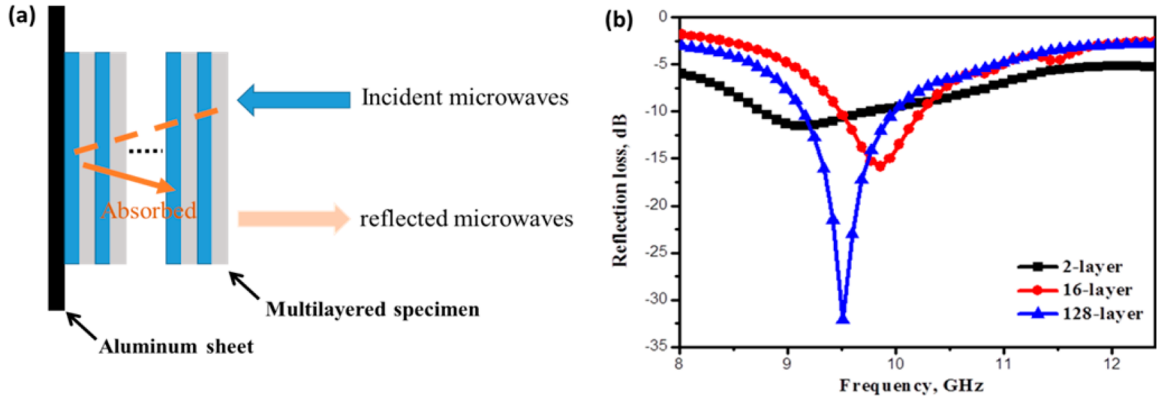

Figure 8. (a) Schematic of the measuring mechanism of microwave absorption ability. (b) Reflection loss of 2-, 16-, and 128-layer PP/PPCB specimens as a function of frequency.

DOI: 10.1021/am506773c
ACS Appl. Mater. Interfaces 2015, 7, 1541−1549

Table 2. Comparison of RL_{max} between PP/PPCB Multilayered Composites and Reported Composites Filled with Carbon-Based Conductive Particles

polymer	filler	configuration	concentration (wt %)	thickness (mm)	RL_{max} (dB)	ref
PP	CB	multilayers	7	1.5	33.3	present work
silicone	CB	single layer	10	1.9	22	42
epoxy	CB	single layer	20	2.7	~25	43
epoxy	CB/SiC	single layer	55	3	41.5	44
epoxy	CF	single layer	15	2	~25	43
PET	CNT	single layer	4	2	17.6	45
PU[a]	CNT	single layer	5	2	22	46
varnish	CNT	single layer	8	1	24.3	45
PVDF	RGO[b]/HT[b]	single layer	5	2	34.9	47
NBR[a]	RGO[b]	single layer	10	3	57	48

[a]PU and NBR are polyurethane and nitrile butadiene rubber. [b]RGO and HT are reduced graphene oxide and hematite, respectively.

sharper and stronger. When the number of layers reaches 128, the peak value even increases to 33 dB. On the basis of the dielectric measurements shown in Figure 7, the material with more layers can promote more electrical charges to accumulate at interfaces. Hence, as a microwave is incident on the dielectric medium, the interfacial polarization would make the main contribution to inherent dissipation of microwave energy.[41]

Table 2 compares the RL_{max} between the present system and some other published composites filled with carbon-based conductive particles. It displays that for reaching a higher absorbing ability most of the systems commonly need more particles. In this work, only 7 wt % CB loading leads the RL_{max} of the multilayered specimen beyond 30 dB. This competitive result is of great importance since the microwave absorbing ability of the whole composites can be strengthened by controlling the distribution of conductive particles, without loading more fillers which may in turn cause deteriorated mechanical properties, processing issues and high costs.

3.4. Mechanical Properties. Apart from competitive microwave absorption ability, favorable mechanical properties are also of great importance for practical application, since the propagation of crazes (or cracks) induced by inorganic particles commonly results in the deterioration of the strength and toughness of the composite material.[28] In this work, tensile tests were performed to explore the influence of the distribution of CB particles on the tensile strength (T_s) and elongation at break (ε_b) of the PP-based composites. As shown in Figure 9, the T_s of the PP/CB conventional specimen is about 23.9 MPa, basically comparable to that of the 128-layer PP/PPCB composite (24.2 MPa). However, the ε_b of the multilayered specimen is beyond 350%, three times larger than that of the conventional one (about 95%). This suggests that a superior mechanical toughness can be achieved through the multilayered distribution of conductive particles. Actually, in conventional system, fillers were randomly distributed in the polymeric matrix. It has been widely reported that crazes (or cracks) originated from those solid particles tended to propagate throughout the whole composite causing the deterioration of mechanical toughness.[49] On the other side, as CB particles were selectively distributed in the multilayered system, a different deforming mechanism was observed. The micrograph inserted in Figure 9 exhibits that the crack originated from the PPCB layer is terminated by the interface and causes numerous scattering crazes (dashed line denotes the scattering zone of crazes) in the adjacent PP layer, which suggests that more energy tends to be consumed in the stretching process leading to a larger elongation before fracturing. This indicates that the multilayered distribution of conductive particles may provide a potential route to fabricate electrical materials with optimal mechanical properties.

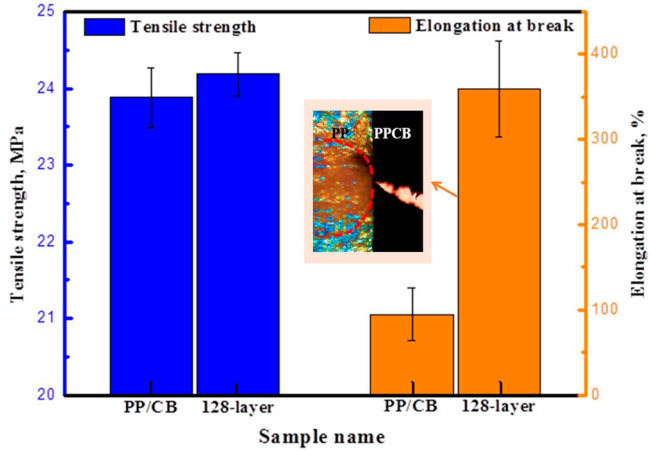

Figure 9. Tensile strength and elongation at break of 128-layer PP/PPCB and PP/CB conventional composites filled with 7 wt % CB (the inserted micrograph is the microstructure of the multilayered specimen observed through PLM).

4. CONCLUSIONS

The well-defined anisotropic alignment of confined CB particles in the PP matrix was fabricated. Considering the specific structure of the multilayered composites, the electrical behaviors were investigated from two different directions: (1) *Parallel to interfaces.* The confined layer space is considered to allow for a more compact connection between CB particles than that in the conventional composite system, promoting the formation of conductive pathways. While further increasing the number of layers, the original conductive network in PPCB layers tends to be broken up due to the separation of insulated PP layers, leading to a distinct enhancement of the electrical resistivity. (2) *Vertical to interfaces.* The multilayered system can be regarded as a "DC block", while the alternating assembly of insulated and conductive layers makes the conductivity become frequency dependent. Thus, the dielectric permittivity is significantly enhanced following the layer multiplication process due to the accumulation of electrical charges at interfaces, which provides a potential application in the microwave absorption. As a microwave is incident on the dielectric medium, the interfacial polarization makes the main contribution on inherent dissipation of microwave energy, so that the

DOI: 10.1021/am506773c
ACS Appl. Mater. Interfaces 2015, 7, 1541−1549

RL becomes strengthened when the material has more layers. Furthermore, tensile behaviors of 128-layer PP/PPCB composite and PP/CB conventional composite were compared. Results exhibit that although the T_s is comparable the ϵ_b of the multilayered system is three times larger than that of the conventional one. The cracks derived from PPCB layers were observed to be terminated by layer interfaces through the craze deflection, which caused more energy consumed in the stretching process leading to a larger extension before fracturing. This indicates that the multilayered distribution of conductive particles may provide a potential route to fabricate electrical materials with optimal mechanical toughness.

AUTHOR INFORMATION

Corresponding Authors

*E-mail: shenjb@scu.edu.cn (Jiabin Shen)
*E-mail: nic7702@scu.edu.cn (Shaoyun Guo).

Notes

The authors declare no competing financial interest.

ACKNOWLEDGMENTS

The authors are grateful to the National Natural Science Foundation of China (51203097, 51227802, 51420105004, 51421061) and the Ministry of Education Priority Funding Areas (20110181130004) for financial support of this work.

REFERENCES

(1) Al-Saleh, M. H.; Sundararaj, U. A Review of Vapor Grown Carbon Nanofiber/Polymer Conductive Composites. *Carbon* **2009**, *47*, 2−22.
(2) Mechrez, G.; Suckeveriene, R. Y.; Zelikman, E.; Rosen, J.; Ariel-Sternberg, N.; Cohen, R.; Narkis, M.; Segal, E. Highly-Tunable Polymer/Carbon Nanotubes Systems: Preserving Dispersion Architecture in Solid Composites via Rapid Microfiltration. *ACS Macro Lett.* **2012**, *1*, 848−852.
(3) Spitalsky, Z.; Tasis, D.; Papagelis, K.; Galiotis, C. Carbon Nanotube−Polymer Composites: Chemistry, Processing, Mechanical and Electrical Properties. *Prog. Polym. Sci.* **2010**, *35*, 357−401.
(4) Yan, J.; Wei, T.; Shao, B.; Ma, F.; Fan, Z.; Zhang, M.; Zheng, C.; Shang, Y.; Qian, W.; Wei, F. Electrochemical Properties of Graphene Nanosheet/Carbon Black Composites as Electrodes for Supercapacitors. *Carbon* **2010**, *48*, 1731−1737.
(5) Mahmoodi, M.; Arjmand, M.; Sundararaj, U.; Park, S. The Electrical Conductivity and Electromagnetic Interference Shielding of Injection Molded Multi-Walled Carbon Nanotube/Polystyrene Composites. *Carbon* **2012**, *50*, 1455−1464.
(6) Stankovich, S.; Dikin, D. A.; Dommett, G. H. B.; Kohlhaas, K. M.; Zimney, E. J.; Stach, E. A.; Piner, R. D.; Nguyen, S. T.; Ruoff, R. S. Graphene-Based Composite Materials. *Nature* **2006**, *442*, 282−286.
(7) Gunes, I. S.; Jimenez, G. A.; Jana, S. C. Carbonaceous Fillers for Shape Memory Actuation of Polyurethane Composites by Resistive Heating. *Carbon* **2009**, *47*, 981−997.
(8) Yu, C.; Kim, Y. S.; Kim, D.; Grunlan, J. C. Thermoelectric Behavior of Segregated-Network Polymer Nanocomposites. *Nano Lett.* **2008**, *8*, 4428−4432.
(9) Xu, X.; Li, Z.; Shi, L.; Bian, X.; Xiang, Z. Ultralight Conductive Carbon-Nanotube−Polymer Composite. *Small* **2007**, *3*, 408−411.
(10) Cao, J.; Zhao, J.; Zhao, X.; You, F.; Yu, H.; Hu, G.; Dang, Z. High Thermal Conductivity and High Electrical Resistivity of Poly(vinylidene fluoride)/Polystyrene Blends by Controlling the Localization of Hybrid Fillers. Compos. *Sci. Technol.* **2013**, *89*, 142−148.
(11) Ameli, A.; Nofar, M.; Park, C. B.; Pötschke, P.; Rizvi, G. Polypropylene/Carbon Nanotube Nano/Microcellular Structures with High Dielectric Permittivity, Low Dielectric Loss, and Low Percolation Threshold. *Carbon* **2014**, *71*, 206−217.
(12) Zeng, Y.; Liu, P.; Du, J.; Zhao, L.; Ajayan, P. M.; Cheng, H. Increasing the Electrical Conductivity of Carbon Nanotube/Polymer Composites by Using Weak Nanotube−Polymer Interactions. *Carbon* **2010**, *48*, 3551−3558.
(13) Li, Y.; Shimizu, H. Conductive PVDF/PA6/CNTs Nanocomposites Fabricated by Dual Formation of Cocontinuous and Nanodispersion Structures. *Macromolecules* **2008**, *41*, 5339−5344.
(14) Gubbels, F.; Blacher, S.; Vanlanthem, E. Design of Electrical Conductive Composites: Key Role of the Morphology on the Electrical Properties of Carbon Black Filled Polymer Blends. *Macromolecules* **1995**, *28*, 1559−1566.
(15) Li, Z.; Xu, X.; Lu, A.; Shen, K.; Huang, R.; Yang, M. Carbon Black/Poly(ethylene terephthalate)/Polyethylene Composite with Electrically Conductive in Situ Microfiber Network. *Carbon* **2004**, *42*, 428−432.
(16) Marin, N.; F, B. Co-Continuous Morphology Development in Partially Miscible PMMA/PC Blends. *Polymer* **2002**, *43*, 4723−4731.
(17) Li, J.; Favis, B. D. Characterizing Co-Continuous High Density Polyethylene/Polystyrene Blends. *Polymer* **2001**, *42*, 5047−5053.
(18) Veenstra, H.; Van Dam, J.; Posthuma De Boer, A. On the Coarsening of Co-Continuous Morphologies in Polymer Blends: Effect of Interfacial Tension, Viscosity and Physical Cross-Links. *Polymer* **2000**, *41*, 3037−3045.
(19) Steinmann, S.; W. G, C. F. Cocontinuous Polymer Blends: Influence of Viscosity and Elasticity Ratios of the Constituent Polymers on Phase Inversion. *Polymer* **2001**, *42*, 6619−6629.
(20) Chaudhry, B. I.; Hage, E.; Pessan, L. A. Effects of Processing Conditions on the Phase Morphology of PC/ABS Polymer Blends. *J. Appl. Polym. Sci.* **1998**, *67*, 1605−1613.
(21) Lee, J.; H, C. Evolution of a Dispersed Morphology From a Co-Continuous Morphology in Immiscible Polymer Blends. *Polymer* **1999**, *40*, 2521−2536.
(22) Xu, X.; Li, Z.; Yang, M.; Jiang, S.; Huang, R. The Role of the Surface Microstructure of the Microfibrils in an Electrically Conductive Microfibrillar Carbon Black/Poly(ethylene terephthalate)/Polyethylene Composite. *Carbon* **2005**, *43*, 1479−1487.
(23) Ogihara, H.; Kibayashi, H.; Saji, T. Microcontact Printing for Patterning Carbon Nanotube/Polymer Composite Films with Electrical Conductivity. *ACS Appl. Mater. Interfaces* **2012**, *4*, 4891−4897.
(24) Hu, P.; Shen, Y.; Guan, Y.; Zhang, X.; Lin, Y.; Zhang, Q.; Nan, C. Topological-Structure Modulated Polymer Nanocomposites Exhibiting Highly Enhanced Dielectric Strength and Energy Density. *Adv. Funct. Mater.* **2014**, *24*, 3172−3178.
(25) Guillaume-Gentil, O.; Zahn, R.; Lindhoud, S.; Graf, N.; Vörös, J.; Zambelli, T. From Nanodroplets to Continuous Films: How the Morphology of Polyelectrolyte Multilayers Depends on the Dielectric Permittivity and the Surface Charge of the Supporting Substrate. *Soft Matter* **2011**, *7*, 3861.
(26) Hewitt, C. A.; Kaiser, A. B.; Roth, S.; Craps, M.; Czerw, R.; Carroll, D. L. Multilayered Carbon Nanotube/Polymer Composite Based Thermoelectric Fabrics. *Nano Lett.* **2012**, *12*, 1307−1310.
(27) Joo, J.; Lee, C. Y. High Frequency Electromagnetic Interference Shielding Response of Mixtures and Multilayer Films Based on Conducting Polymers. *J. Appl. Phys.* **2000**, *88*, 513−518.
(28) Chen, B.; Gao, W.; Shen, J.; Guo, S. The Multilayered Distribution of Intumescent Flame Retardants and Its Influence on the Fire and Mechanical Properties of Polypropylene. *Compos. Sci. Technol.* **2014**, *93*, 54−60.
(29) Shen, J.; Wang, M.; Li, J.; Guo, S.; Xu, S.; Zhang, Y.; Li, T.; Wen, M. Simulation of Mechanical Properties of Multilayered Propylene-Ethylene Copolymer/Ethylene 1-Octene Copolymer Composites by Equivalent Box Model and Its Experimental Verification. Euro. *Polym. J.* **2009**, *45*, 3269−3281.
(30) Zhang, M. Q.; Yu, G.; Zeng, H. M.; Zhang, H. B.; Hou, Y. H. Two-Step Percolation in Polymer Blends Filled With Carbon Black. *Macromolecules* **1998**, *31*, 6724−6726.
(31) Sumita, M.; Sakata, K.; Hayakawa, Y.; Asai, S.; Miyasaka, K.; Tanemura, M. Double Percolation Effect on the Electrical

DOI: 10.1021/am506773c
ACS Appl. Mater. Interfaces 2015, 7, 1541−1549

Conductivity of Conductive Particles Filled Polymer Blends. *Colloid Polym. Sci.* **1992**, *270*, 134−139.
(32) Zhang, J.; Mine, M.; Zhu, D.; Matsuo, M. Electrical and Dielectric Behaviors and their Origins in the Three-Dimensional Polyvinyl Alcohol/MWCNT Composites with Low Percolation Threshold. *Carbon* **2009**, *47*, 1311−1320.
(33) Zhu, L.; Wang, Q. Novel Ferroelectric Polymers for High Energy Density and Low Loss Dielectrics. *Macromolecules* **2012**, *45*, 2937−2954.
(34) Dang, Z.; Yuan, J.; Zha, J.; Zhou, T.; Li, S.; Hu, G. Fundamentals, Processes and Applications of High-Permittivity Polymer−Matrix Composites. *Prog. Mater. Sci.* **2012**, *57*, 660−723.
(35) Bobrov, V. B.; Trigger, S. A. The True Dielectric and Ideal Conductor in the Theory of the Dielectric Function of the Coulomb System. *J. Phys. A: Math. Theor.* **2010**, *43*, 365002.
(36) Jonscher, A. K. Dielectric Relaxation in Solids. *J. Phys. D: Appl. Phys.* **1999**, *32*, R57−R70.
(37) Yousefi, N.; Sun, X.; Lin, X.; Shen, X.; Jia, J.; Zhang, B.; Tang, B.; Chan, M.; Kim, J. Highly Aligned Graphene/Polymer Nanocomposites with Excellent Dielectric Properties for High-Performance Electromagnetic Interference Shielding. *Adv. Mater.* **2014**, *26*, 5480−5487.
(38) Cao, M.; Song, W.; Hou, Z.; Wen, B.; Yuan, J. The Effects of Temperature and Frequency on the Dielectric Properties, Electromagnetic Interference Shielding and Microwave-Absorption of Short Carbon Fiber/Silica Composites. *Carbon* **2010**, *48*, 788−796.
(39) Li, N.; Huang, Y.; Du, F.; He, X.; Lin, X.; Gao, H.; Ma, Y.; Li, F.; Chen, Y.; Eklund, P. C. Electromagnetic Interference (EMI) Shielding of Single-Walled Carbon Nanotube Epoxy Composites. *Nano Lett.* **2006**, *6*, 1141−1145.
(40) Liu, Z.; Bai, G.; Huang, Y.; Ma, Y.; Du, F.; Li, F.; Guo, T.; Chen, Y. Reflection and Absorption Contributions to the Electromagnetic Interference Shielding of Single-Walled Carbon Nanotube/Polyurethane Composites. *Carbon* **2007**, *45*, 821−827.
(41) Wang, D.; Bao, Y.; Zha, J.; Zhao, J.; Dang, Z.; Hu, G. Improved Dielectric Properties of Nanocomposites Based on Poly(vinylidene fluoride) and Poly(vinyl alcohol)-Functionalized Graphene. *ACS Appl. Mater. Interfaces* **2012**, *4*, 6273−6279.
(42) Kwon, S. K.; Ahn, J. M.; Kim, G. H.; Chun, C. H.; Hwang, J. S.; Lee, J. H. Microwave Absorbing Properties of Carbon Black/Silicone Rubber Blend. *Polym. Eng. Sci.* **2002**, *42*, 2165−2171.
(43) KIM, J.; LEE, S.; KIM, C. Comparison Study on the Effect of Carbon Nano Materials for Single-Layer Microwave Absorbers in X-Band. Compos. *Sci. Technol.* **2008**, *68*, 2909−2916.
(44) Liu, X.; Zhang, Z.; Wu, Y. Absorption Properties of Carbon Black/Silicon Carbide Microwave Absorbers. *Compos. Part B: Eng.* **2011**, *42*, 326−329.
(45) Fan, Z.; Luo, G.; Zhang, Z.; Zhou, L.; Wei, F. Electromagnetic and Microwave Absorbing Properties of Multi-Walled Carbon Nanotubes/Polymer Composites. *Mater. Sci. Eng., B* **2006**, *132*, 85−89.
(46) Liu, Z.; Bai, G.; Huang, Y.; Li, F.; Ma, Y.; Guo, T.; He, X.; Lin, X.; Gao, H.; Chen, Y. Microwave Absorption of Single-Walled Carbon Nanotubes/Soluble Cross-Linked Polyurethane Composites. *J. Phys. Chem. C* **2007**, *111*, 13696−13700.
(47) Chen, D.; Quan, H.; Huang, Z.; Luo, S.; Luo, X.; Deng, F.; Jiang, H.; Zeng, G. Electromagnetic and Microwave Absorbing Properties of RGO@Hematite Core−Shell Nanostructure/PVDF Composites. *Compos. Sci. Technol.* **2014**, *102*, 126−131.
(48) Singh, V. K.; Shukla, A.; Patra, M. K.; Saini, L.; Jani, R. K.; Vadera, S. R.; Kumar, N. Microwave Absorbing Properties of a Thermally reduced Graphene Oxide/Nitrile Butadiene Rubber Composite. *Carbon* **2012**, *50*, 2202−2208.
(49) Ha, H. W.; Choudhury, A.; Kamal, T.; Kim, D.; Park, S. Effect of Chemical Modification of Graphene on Mechanical, Electrical, and Thermal Properties of Polyimide/Graphene Nanocomposites. *ACS Appl. Mater. Interfaces* **2012**, *4*, 4623−4630.

DOI: 10.1021/am506773c
ACS Appl. Mater. Interfaces 2015, 7, 1541−1549